ORIGINAL PAPER

Microstructural properties and compressive strength of fly ash-based geopolymer cement immersed in CO_2-saturated brine at elevated temperatures

S. Ridha[1,2] · **I. Dzulkarnain[1]** · **M. Abdurrahman[3]** · **S. U. Ilyas[2]** · **M. Bataee[4]**

Abstract

Geopolymer cement has significance in several engineering applications due to improved physical and chemical characteristics compared to ordinary portland cement (OPC). However, the emphasis on petroleum industry for cementing is not well recorded under CO_2 exposure. This experimental research aims to investigate the impact of CO_2-saturated brine on geopolymer-based and OPC-based cement under elevated temperature. Fly ash-based alkali-activated cement is prepared, and cement slurry is cured at two different conditions (17.23 MPa/60 °C and 24.13 MPa/130 °C). The slurry is then submerged into CO_2-saturated brine using autoclave chamber at supercritical CO_2 conditions for 24, 72 and 96 h. Microstructure properties are characterized using SEM, XRF, XRD, and IR. Compression strength is experimentally tested on cubical cement samples. A comparative analysis of fly ash geopolymer cement and OPC at varying conditions exhibits that microstructure and compressive strength of geopolymer cement show better performance. It signifies the potential of fly ash as a binder in sequestration cement for CO_2 injection wells. This research suggests that the concentration of CO_2 has a minor influence on the degree of carbonation. However, the temperature is found to be a critical factor for microstructure and mechanical properties reduction in OPC in a CO_2-rich environment.

Keywords Alkali-activated cement · Compressive strength · Fly ash · Geopolymer · Microstructure · Supercritical CO_2

Abbreviations

C_3S (Alite)	Tricalcium silicate
C_2S (Belite)	Dicalcium silicate
C_3A	Tricalcium aluminate
C_4AF	Tetracalcium aluminoferrite
GC60	Geopolymer cement cured at 60 °C and 17.23 MPa
GC130	Geopolymer cement cured at 130 °C and 24.13 MPa
PC60	Class G cement cured at 60 °C and 17.23 MPa
PC130	Class G cement cured at 130 °C and 24.13 MPa
96GC130b	Geopolymer cement after brine CO_2 exposure at 130 °C and 24.13 MPa for 96 h
96PC130b	Class G cement after brine CO_2 exposure at 130 °C and 24.13 MPa for 96 h
72GC60b	Geopolymer cement after brine CO_2 exposure at 60 °C and 17.23 MPa for 72 h
72PC60b	Class G cement after brine CO_2 exposure at 60 °C and 17.23 MPa for 72 h
24GC130b	Geopolymer cement after brine CO_2 exposure at 130 °C and 24.13 MPa for 24 h
24PC130b	Class G cement after brine CO_2 exposure at 130 °C and 24.13 MPa for 24 h

✉ S. Ridha
syahrir.ridha@utp.edu.my

1 Petroleum Engineering Department, Universiti Teknologi PETRONAS, 32610 Seri Iskandar, Perak, Malaysia

2 Institute of Hydrocarbon Recovery, Universiti Teknologi PETRONAS, 32610 Seri Iskandar, Perak, Malaysia

3 Petroleum Engineering Department, Universitas Islam Riau, 28284 Kota Pekanbaru, Riau, Indonesia

4 Petroleum Engineering Department, Curtin University Malaysia, 98009 Miri, Sarawak, Malaysia

🖄 Springer

Introduction

The cementing sector is widely recognized in several engineering industries involving chemical, mechanical, petroleum, and construction. The demand for cement is increasing globally, which drastically increases CO_2 production as well. It is an alarming scenario that requires mitigation plans to minimize CO_2 emissions from the cement industries. The researchers in recent years have proposed the solution that clinker-free cement can be an alternative to reduce the emissions. The other significant option is partly replacement of portland cement by other supplementary cementitious materials. Petroleum exploration cementing (oil and gas well) is one of the crucial processes in post-drilling operation when the drilling reaches the target depth, and the casing string has been set up in place. The cement slurry is introduced in between the annular space of the wellbore and casing or two casing strings. The primary target of a wellbore cementing is to prevent fluid movement between zones and support casing, as an effort to create efficient wellbore integrity. For this purpose, well cement should meet the required characteristics such as long-term integrity, less permeable, non-shrinking, able to withstand compressive and tensile loads, and resistance to an acidic environment (H_2S, CO_2, also referred to as acid gas). It also has good bonding with casing formation and not harmful to casing integrity (Khalifeh et al. 2014). The wellbore integrity is the most crucial parameter in the well-cementing process, which is highly dependent on the characteristics of cement slurry (Velayati et al. 2015).

Class G cement (OPC-based cement) is the most commonly used cement in the petroleum exploration sectors due to the ability to be mixed with a wide range of additives (Ridha et al. 2013; Mahmoud et al. 2018). However, the primary concern is that OPC-based cement is not stable in rich CO_2 acid reservoirs (Santra et al. 2009; Kutchko et al. 2008; Zhang et al. 2013; Omosebi et al. 2017). It may rise to wells integrity problems due to fluids leak paths. As a result, it can lead to the contamination of freshwater by reservoir fluid, charged formation pressure, or even fluids kick-out from the formation. Few studies are found in the literature (Kutchko et al. 2008; Sauki and Irawan 2010; Jacquemet et al. 2012; Chindaprasirt et al. 2013) on the interactions between CO_2, neat cement, and pozzolanic material. It was observed that several oil wells were cemented using a mixture of Class G and pozzolanic additives. However, not much investigation has been conducted to inspect the interactions between CO_2, brine, and geopolymer cement under elevated temperature conditions. Calcium carbonate and solid carbonates (e.g., calcite, aragonite, or vaterite) can react with CO_2-formed calcium bicarbonate. It can lead to high porosity, high permeability, and lower compressive strength of the cement paste (Omosebi et al. 2016; Ridha et al. 2018).

Geopolymer cement is usually formed as a reaction of highly concentrated aqueous alkali hydroxide or silicate solution with the aluminosilicate solid source materials (Davidovits 2011; Junaid et al. 2017). The aluminosilicate source materials consist of fly ash, silica fume, metakaolin, granulated blast furnace slag, and rice husk ash (Ramezanianpour 2014). Geopolymer cement is known to have improved and efficient properties and affective characteristics of cement, such as high compressive strength, low shrinkage, excellent resistance to sulfate attack, good acid resistance, and low creep depending on the raw material selection and curing conditions (Palomo et al. 1999; Phair and Deventer 2002). A mixture of alkali hydroxide and silicate solution, commonly known as an alkali activator, in general, is a combination of sodium hydroxide or potassium hydroxide with sodium silicate or potassium silicate (Duxson et al. 2007). An alkali hydroxide solution is required for the dissolution of raw materials, while sodium (or potassium) silicate solution acts as a binder, alkali activator, and dispersant (Junaid et al. 2017). A recent study by Zhang et al. (Zhang et al. 2020) concluded that the geopolymers synthesized by the binary mixtures of glass powder and slag with high calcium content achieved much higher compressive strength, and the appropriate increase in curing temperature had a more positive impact on the mechanical properties of geopolymers made with glass powder. Kaze et al. (2020) studied the reaction kinetics and rheological behavior of meta-halloysite-based geopolymer cured at room temperature. It was found that the increase in calcination temperature from 600 to 750 °C considerably improved the reactivity of halloysite clay by the increase in the amount of amorphous phase within meta-halloysite. In another recent study by Ridha et al. (2020), wet supercritical CO_2 was injected on fly ash geopolymer cement under elevated temperatures for well cement applications. It was found that the strength development continues to build up under elevated temperature and pressure by producing zeolite which is beneficial as a filler in a pore.

Geopolymer cement is one of the most trending areas of research in the current era due to its vast application in construction industries. The researchers have shown significant interest in geopolymer cement due to the efficient chemical and physical properties compared to Class G cement. However, limited knowledge is available in the literature, especially the applications to the oil and gas industry for cementing jobs that are not well recorded under CO_2 exposure at reservoir conditions. This research paper aims to experimentally investigate the impact of CO_2-saturated brine on geopolymer cement under elevated temperature and pressure (reservoir conditions). The study focuses on the characteristics of fly ash geopolymer cement and Class G cement before and after exposure to CO_2-saturated brine. These experimental characteristics include mineralogical composition,

microstructure behavior, and compressive strength. The literature suggests several investigations on microstructure and compressive strength of geopolymers derived from different sources (Belmokhtar et al. 2017). To the authors' knowledge, the microstructural and compressive strength of geopolymer cement under the curation of CO_2-saturated brine and high temperature has not been subjected to investigation, hence establishing the novelty of this research. The previous studies are mostly focused on the investigations at standard room conditions. However, in this study, the curing process CO_2-saturated brine is performed for 24 h with two different pressure/temperature conditions (17.23 MPa/60 °C and 24.13 MPa/130 °C), which has significance in the oil and gas exploration sectors. The alkali/fly ash ratio in this research is selected based on optimum ratio provided by the literature (Duxson et al. 2007; Belmokhtar et al. 2017; Nuruddin et al. 2011; Ridha and Yerikania 2015), and the API 13 B (American Petroleum Institute) standard variation is used for the slurry preparation. Therefore, the variation in alkali/fly ash ratio or cement slurry is not considered in this work.

Materials and methods

Materials

The principal materials for this research are fly ash, Class G cement, sodium silicate solution, and sodium hydroxide pellets. Fly ash is collected from the by-product produced by Tenaga Nasional Berhad (TNB) Manjung Power Plant, Malaysia. X-ray fluorescence (XRF) analysis is performed to find the chemical compositions of fly ash and Class G cement powder. The compositions are given in Table 1. It is found that the combined quantity of oxides containing silica, iron, and aluminum in fly ash and Class G cement powder samples corresponds to 68.2% and 32.68%, respectively. The chemical analysis from XRF exhibits a minute quantity of unreacted fly ash that can be categorized as Class C fly ash.

Preparation and curing of fly ash geopolymer cement

Alkali activator/fly ash ratio

The literature review (Duxson et al. 2007; Belmokhtar et al. 2017; Nuruddin et al. 2011; Ridha and Yerikania 2015) suggests that the ratio of alkali activator to fly ash can be set at 0.44. The previous study by Ridha et al. (2015) justifies that this alkali activator-to-fly ash ratio contributes to the highest compressive strength. The ratio of sodium hydroxide to sodium silicate is also fixed at 2.5 for this investigation. An alkali activator solution is prepared by diluting a definite amount of sodium hydroxide pellets in distilled water in such

Table 1 Composition of fly ash and Class G cement powder

Compositions	Fly ash	Class G cement powder
CaO (%)	20.70	64.8
SiO_2 (%)	32.40	24.10
Al_2O_3 (%)	12.20	3.85
Fe_2O_3 (%)	23.60	4.73
TiO_2 (%)	1.38	0.086
K_2O (%)	2.02	0.091
MgO (%)	2.35	0.346
Na_2O (%)	0.87	0
P_2O_5 (%)	0.86	0.224
SO_3 (%)	2.40	1.36
Others (%)	1.22	0.413

a way that the concentration of sodium hydroxide is 8 molal solution. Both sodium hydroxide and sodium silicate are weighed in accordance with the predetermined mass.

Cement slurry preparation

The ratio of water to Class G cement was fixed at 0.44, and the samples are prepared according to the API RP 10A (Recommended Practice and 10A 2011) and API RP 10B-2 (API Recommended Practice 2009) standards. Geopolymer cement slurry is prepared by gently pouring sodium silicate into the mixer filled with 8 molal sodium hydroxide solution for approximately 10 s. The fly ash is then poured into alkali solution with a speed mixer for 15 s at 4000 rpm, and the mixing is further continued for 35 s at 12,000 rpm to obtain a homogeneous slurry.

Curing and specimen preparation

After preparing the cement slurry with required standards, the slurry is poured into a $2 \times 2 \times 2$-inch steel cubic mold, which is coated with grease. The molds are then located inside a high-pressure, high-temperature (HPHT) curing chamber containing a pressure vessel with controlled heating rates. The curing process is performed for 24 h with two different pressure/temperature conditions, i.e., 17.23 MPa/60 °C and 24.13 MPa/130 °C, to prepare cement paste for CO_2-saturated brine immersion experiments. The mix design preparation of geopolymer cement samples used in this experimental study is shown in Table 2. Here, GC60 corresponds to geopolymer cement cured at 60 °C and 17.23 MPa, whereas GC130 corresponds to geopolymer cement cured at 130 °C and 24.13 MPa. Similarly, PC60 is abbreviated for the

Table 2 Mix design of geopolymer cement

No.	Identification	NaOH molality (m)	Curing temperature ($^\circ$C)	Curing pressure (MPa)
1	GC60	8	60	17.24
2	PC60	–	60	17.24
3	GC130	–	130	24.13
4	PC130	–	130	24.13

OPC-based Class G cement cured at 60 °C and 17.23 MPa, and PC130 corresponds to OPC-based Class G cement cured at 130 °C and 24.13 MPa.

The degradation testing is performed for the obtained hardened cement. Geopolymer cement and Class G cement paste were cured at 17.23 MPa/60°C and 24.13 MPa/130°C immersed in CO_2-saturated brine solution in a 7.5-L (Hastelloy C-276) HP/HT dynamic autoclave (120 mm diameter × 570 mm depth). The autoclave vessel is capable of handling operations up to 35 MPa and 300 °C. A booster pump is used to charge low-pressure CO_2 gas from vessel to autoclave via a small diameter pipe made of stainless steel. The temperature is controlled by an AC12T controller with an accuracy of ± 1 °C.

Geopolymer and Class G cement pastes are soaked in 3% NaCl solution (acting as a brine) saturated with CO_2 under elevated temperature and pressure conditions. The cement carbonation due to the CO_2 exposure tests is conducted by placing hardened cement paste and brine solution inside a cement autoclave. The vessel is then pressurized with CO_2 gas to resemble reservoir HP/HT conditions, i.e., 17.23 MPa/60 °C and 24.13 MPa/130 °C. A pH measurement analysis is performed initially for 3% brine solution, exhibiting a value of 5.97. CO_2-saturated brine condition is obtained by continuously injecting CO_2 gas into brine for approximately 2 h. The pH of CO_2-saturated brine is set in the range of 3.8–4.0, and the measurement is concluded at 23 °C (± 2 oC) at 1.01 MPa. The CO_2 is in a supercritical state at predetermined temperatures and pressures. Inside the cement autoclave, samples are arranged in a stack for the identification of submerged and non-submerged cement samples in the brine solution. This arrangement assists in investigating the impact of carbonation to cement paste after exposure to the CO_2-saturated brine. The experiments are performed in a controlled CO_2-saturated brine environment with a controlled heat rates as a function of high-temperature/high-pressure environment. The tests are performed under three different static conditions, i.e., 24, 72, and 96 h, to determine the effect of acid gas deterioration on cement pastes cured at discrete conditions. At the end of each test, autoclave pressure is reduced gradually for 1 to 2 hours to hinder sample breakage.

Experimental testing and characterizations

Material characterization

The degradation of the cement after exposure to CO_2-saturated brine under elevated temperature and pressure for 24, 72, and 96 h is studied using different characterization techniques. These techniques include scanning electron microscopy (SEM), X-ray fluorescence (XRF), X-ray diffraction (XRD), and infrared spectroscopy (FTIR). Electron microscopy analysis is performed using field emission SEM (FESEM), SUPRA55VP, Germany. This analysis is used for microstructural observations of the affected surfaces. For microstructure analysis, the fragments are collected at 1–2 mm depth from the sample surface under an acceleration voltage of 10 kV. The observation is performed at a working distance (WD) of 3–10 mm. The observed samples are coated with evaporated gold before investigation using the secondary electron mode of the FESEM. The XRF characterization provides the sample element percentage. The SEM analysis is used for the visual appearance of different phases inside the sample from millimeters to micron meters to produce information such as an excellent physical and mechanical description of the crystalline microstructure and amorphous materials (Komnitsas and Zaharaki 2007). XRD analyses are performed using PAN analytical XPERT3 powder diffractometer with specific configurations. The investigation is conducted at a continuous 2θ (degree) scan range of 5°-80° with a scan step of 0.01. A fixed divergent slit of 0.38 mm is used, and the Kα value is fixed at 1.54. The generator voltage and the current are set to be 45 kV and 40 mA, respectively. FTIR spectroscopy is an analytical method used to identify the presence of different functional groups and to determine the major reaction zones of Si–O and Al–O of cementitious paste (Ryu et al. 2013). PerkinElmer Spectrum One/BX spectrometer is employed for FTIR analysis with a wave range of 400–4000 cm^{-1}.

Compressive strength

The compressive strength of the geopolymer cement is measured according to ASTM C 109 (ASTM C 2008) using an ELE ADR 3000 with a capacity of 3000 kN on the 2-inch cubical samples. For each sample set, the compressive strength tests are conducted on three cubical samples separately, and the average values are reported.

Results and discussion

SEM analysis

Electron microscopy analysis is performed for different cement samples immersed in CO_2-saturated brine for 72 and

96 h, as shown in Fig. 1a–d that corresponds to 72GC60b, 72PC60b, 96GC130b, and 96PC130b samples, respectively. The effect of CO_2-saturated brine on Class G cement is shown in Fig. 1a, b, and the impact on geopolymer cement is presented in Fig. 3c, d. It is evident from Fig. 1 that aragonite (calcium carbonate, C), a small amount of ettringite (E), and most of the amorphous SiO_2 (S) are present in the sample. Furthermore, approximately all content of calcium hydroxide (P) is transformed into aragonite due to the carbonation in the presence of carbonic acid. The presence of calcium hydroxide is still visible despite after carbonation during the immersion test for 96 h at 130 °C, evident in Fig. 1b. The presence of calcium hydroxide in the cement acts as a primary defense against carbonic acid by maintaining a pH of 12.0 inside the pore. Calcium hydroxide is dissolved by carbonic acid due to acid diffusion into the pore, producing calcium carbonate. The pH of the system decreases when calcium hydroxide is fully depleted. It is attributed to the failure of the buffer system inside the pore cement. Then, carbonic acid begins to attack C–S–H gel and then convert C–S–H gel phase into calcium carbonate and amorphous silica gel (complete carbonation) or calcium silicate carbonate, C–S–C (incomplete carbonation).

It is evident from Fig. 1c that geopolymer cement exhibits a porous structure after 96 h of exposure to CO_2-saturated brine. Furthermore, 96GC130b is observed to be highly porous and fragile in the surface area after the immersion on CO_2-saturated brine. A half-spherical concave shape is identified on the sample surface with a diameter in the range of 0.5–2 μm. A few pores and micro-cracks are also visible in the sample. However, it is challenging to justify the actual reason for crack formation. It can either be due to the carbonation or force effects outside the compressive strength test. Aragonite (calcium carbonate, C) is a new crystal that can be seen inside some of the pores indicated in Fig. 1d. The hollow spheres of fly ash react with the alkaline activator solution to yield gel, which is identified as Si–O–Al and Si–O–Si bonds. Geopolymerization between fly ash and alkali activator is induced by the availability of Al and Si in both reactants. Partially reacted or unreacted fly ash particles create cavities, dispersed small size of pores, in the surface of the cement gel matrix. Larnite, ettringite, and aragonite are formed as a newly detected crystal that fills the pores based on the physical appearance and chemical composition of raw materials, as shown in Fig. 1d.

Chemical composition

XRF analysis is performed to quantify the chemical composition of the samples. It is found that the element content of Si, Fe, and Al in fly ash constitutes to 68.2%. The Ca content of fly ash is approximately 20.7%, categorized as high-calcium fly ash. In terms of the geopolymerization, Si and Al react with an alkaline activator solution to yield an aluminosilicate framework, which is represented by Si–O–Al–O–Si bonds. It is also observed that fly ash with high calcium content leads to higher reactivity compared to fly ash with low calcium content, and it is noticeable due to

Fig. 1 SEM image of samples after CO_2-saturated brine exposure at specific duration: **a** 72PC60b, **b** 96PC130b, **c** 72GC60b, and **d** 96GC130b. The abbreviations refer to portlandite/calcium hydroxide (P), silica (S), calcium carbonate (C), and ettringite (E)
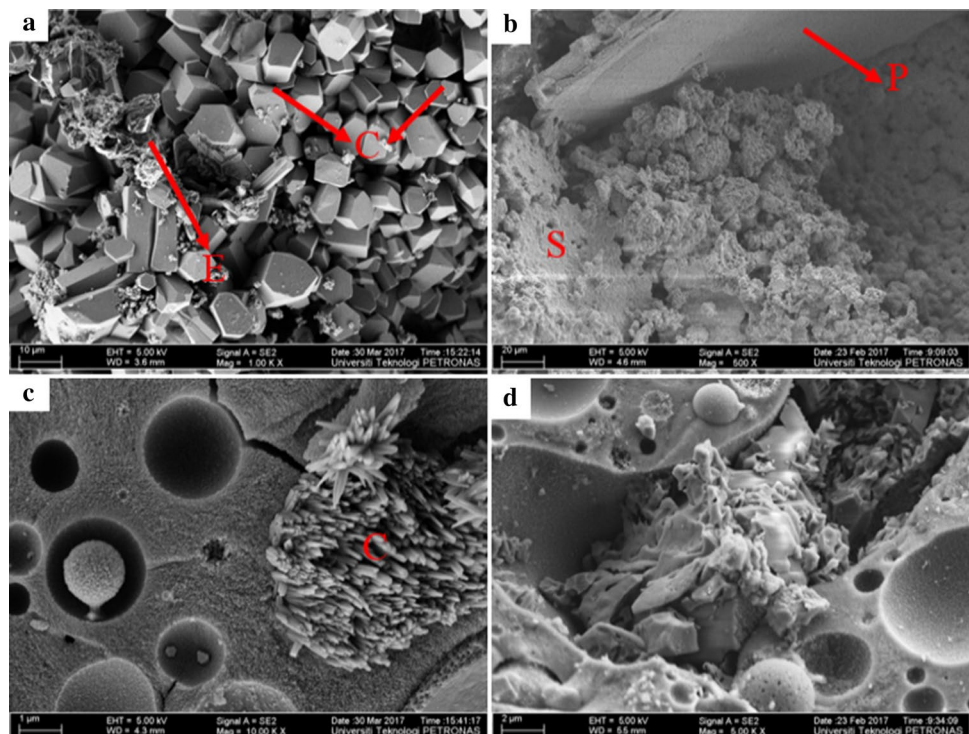
the short thickening time in alkali-activated paste measured using consistometer. The fly ash has low alkali (Na_2O) content, which illustrates that the fly ash is not much reactive compared to other alkalis. The increase in pH of the solution inside the cement pore affirms that it does not hasten the fly ash dissociation or alkali silica reaction (ASR) (Fauzi et al. 2016). The oxides composition of Class G cement powder indicates that Al/Fe ratio is less than 0.64, and the proportions of C_3S, C_2S, C_3A, and C_4AF using Bogue calculation are 60.0, 23.8, 1.3, and 14.9%, respectively. C_3S and C_2S are responsible for strength development, initial strength gain and strength gain after 7 days. Due to the shallow content of C_3A phase (below 2%), it can be categorized as cement with high sulfate resistance. Although C_4AF hydrates rapidly, it does not increase much on strength development of the cement.

XRD analysis

The diffractogram of fly ash and geopolymer cement paste after 24-h curing is shown in Fig. 2. The analysis is performed with an inset sample scanned using different configurations consisting of anti-scatter and divergence slit, step size, and counting time. The samples are scanned using low counting time, larger step size, and smaller slit to obtain short peaks with low intensity. It is also challenging to differentiate between small peaks and noises. Diffractograms with the configuration of 100 s counting time and 1/8 slit depicted only six peaks that are identified, and other peaks are found to be challenging to distinguish between the peak and the noise. Therefore, the optimum combination at 500 s counting time, 0.01 step size, and 1/4 slit is selected to obtain good peaks with intensity at more than 2500 counts.

The diffractogram of fly ash and alkali-activated cement paste after 24-h curing is shown in Fig. 2. The fly ash sample illustrates peaks at 12° and 25.5° corresponding to kaolinite and anhydrite, that are vanished in GC60 and GC130 samples. This is attributed to the reason that the crystal surface is masked by the amorphous phases through the reaction of aluminosilicate framework with atmospheric CO_2 or by an ordinary product of geopolymerization producing Si–O–Al–O–Si framework, thereby covering the XRD reflections of the mullite. Therefore, the peaks of kaolinite, anhydrite, or other crystalline material are absent. Peaks due to the crystalline component of fly ash (quartz, Q; magnetite, Mg; hematite, H; mullite, M; anhydrite, A) can be seen in the region of 16° to 40° arising from the glassy phase of the fly ash. The crystals identified from the diffractogram of fly ash and geopolymer cement cured at 60 °C and 130 °C are shown in Fig. 2. It is observed that three similar peaks are found in region 26.6°, 33.3°, and 35.6° in GC60 and GC130, which can be identified as phases of quartz, mullite, and magnetite. A comparison between fly ash and GC60
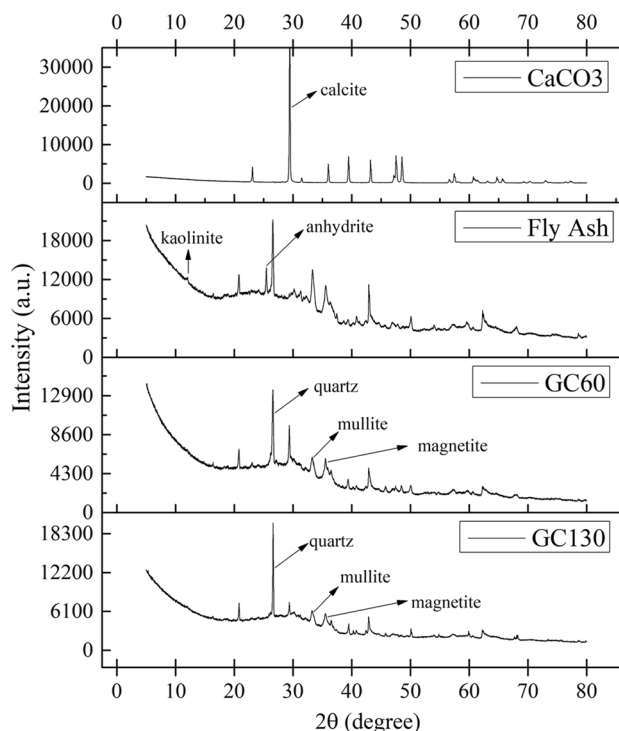

Fig. 2 Diffractogram of fly ash and alkali-activated cement paste after 24-h curing

diffractogram reveals that peaks located at 12° (kaolinite) and 25.4° (anhydrite) initially exist in fly ash. It suggests that kaolinite encounters a dissolution and polycondensation forming Si–O–Al–O–Si framework in the presence of alkali activator, and white anhydrite transforms into ettringite.

A comparison of calcium carbonate, Class G cement, PC 60 and PC 130 after 24 h of curing is shown in Fig. 3. The dominant phases in Class G cement powder (C_3S, C_2S, C_3A and C_4AF) are indicated in Fig. 3. It is observed that the peaks overlap between each phase of 2–3 polymorphs, i.e., C_2S has polymorph as alpha-, beta-, and gamma-C_2S. A similar XRD pattern is also observed between the cement hydration product and the cement clinker; for example, between calcite and alite there is a similar peak at 39.4°.

A comparative XRD pattern of geopolymer cement cured at 60 °C and 130 °C immersed in CO_2-saturated brine for 24, 72 and 96 h is shown in Fig. 4. The samples exhibit a similar generalized pattern. The differences appear on diffractogram of samples under curing temperature of 130 °C, located at 2θ of 12.5°, 17.8°, 21.7° and 28.1° identified as gismondine (sodium alumina silicate hydrate, NASH) crystal. The N-peaks that belong to gismondine crystal are not indicated in diffractogram of GC60 and GC130 (cement before CO_2 exposure) and also for samples exposed to CO_2 at 60 °C. It can be concluded that NASH was produced during CO_2-saturated brine exposure of geopolymer cement. Significant transformations in XRD diffractogram of
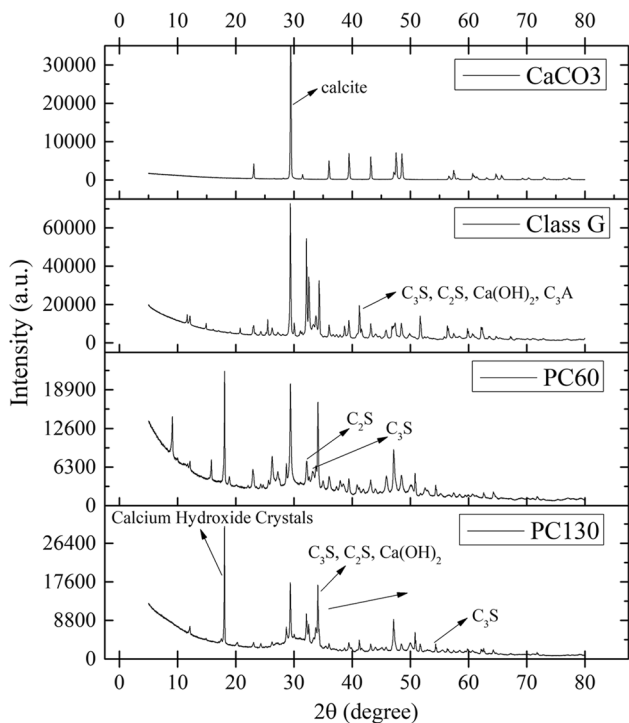
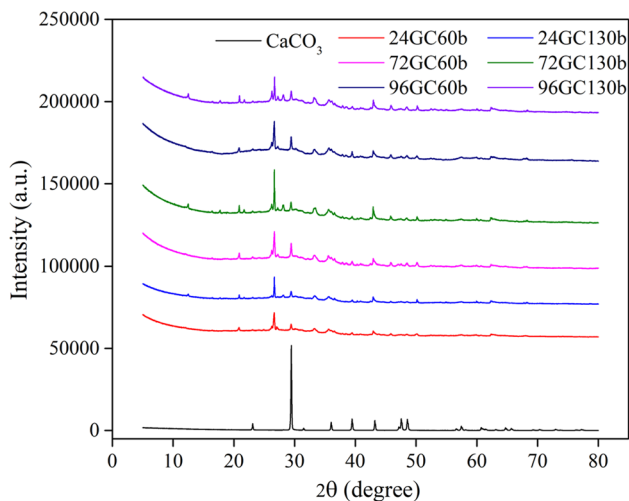**Fig. 3** XRD pattern of portland cement (PC) paste after 24-h curing

Fig. 4 XRD pattern of the alkali-activated cement cured after exposed to CO_2-saturated brine at 60 °C and 130 °C

geopolymer cement after CO_2-saturated brine exposure at 60 °C are identified as the formation of calcium carbonate.

FTIR analysis

The FTIR spectrum of the fly ash, GC60, GC130, and cement paste after CO_2-saturated brine exposure at the band range of 400–4000 cm^{-1} is compared in Fig. 5. Several absorption frequencies in the range of 960–1010 cm^{-1}

are indicated which affirms that the transformation occurs during geopolymerization. The broad spectrum in all infrared bands in the range of 1600 to 3500 cm^{-1} is identified to stretching and bending vibrations of H–O–H bond from molecules of water entrapped in the pore, which is then absorbed on the surface of the pore or attached in the spacious hollow of the aluminosilicate framework. The higher values of these bands indicate that more mass of water molecule is absorbed in Si–O–Si bending vibrations by the spectra below 500 cm^{-1}. The formation of semicrystalline or an amorphous alumina silicate phase of the materials is observed at a band range 500–800 cm^{-1}, which exhibits the symmetric stretching vibration of the Si–O–Si and Si–O–Al bonds. An increasing profile of Si–O–Si bond in the sample can be seen at the band range 1600–1000 cm^{-1}. FTIR spectra of Si–O–C bond of fly ash, GC60, and GC130 are found at 1019 cm^{-1}, 1003 cm^{-1}, and 965.3 cm^{-1}, respectively. These spectrums indicate that the glassy component of the aluminosilicate source material reacting with alkali activator solution produces aluminosilicate gel as indicated by Si–O–Si and Si–O–Al bonds. Si–O–Si and Si–O–Al spectra of samples cured at 130 °C are shifted to the lower frequency compared to the samples cured at 60 °C. The stretching modes are sensitive to the Si–Al composition in the framework of alkali activated due to an increasing number of tetrahedral aluminum atoms. A similar pattern of Si–O–C bond is also found in geopolymer cement (GC) paste after immersed in CO_2-saturated brine at temperature 60 °C. The Si–O–Si bond of 24GC60b, 72GC60b, and 96GC60b is located at 1009 cm^{-1}, 1009 cm^{-1} and 1006 cm^{-1} (shown in the gray-shaded area). The samples exposed at 96 h have the lowest
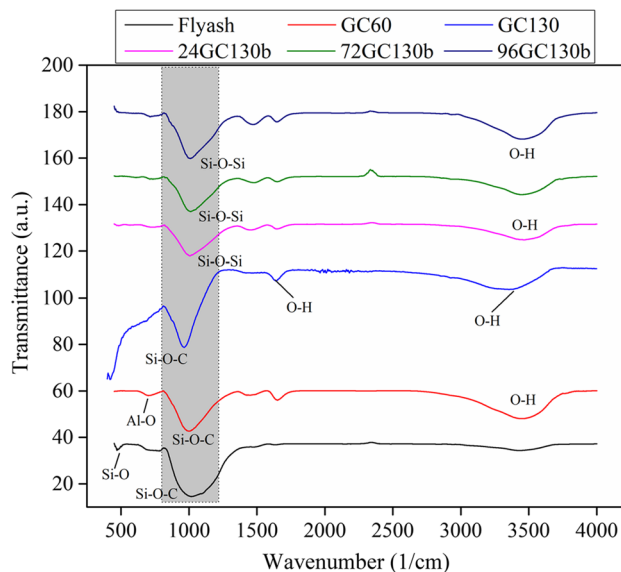

Fig. 5 FTIR pattern of the fly ash and alkali-activated cement (GC) paste before and after exposure to CO_2-saturated brine

frequency located at 1006 cm^{-1}. The Si–O–Si bond exposed under 130 °C at a wavenumber of 1015 cm^{-1} indicates that strength development is occurring. This analysis affirms that the product consists of more Si–O–Si and Si–O–Al bonds than other samples, which is causing higher compressive strength (Bakria et al. 2011).

A comparative IR spectrum of Class G cement powder, PC60 and PC130 before and after CO_2-saturated brine exposure at band range 400–4000 cm^{-1} is presented in Fig. 6. It is found that the peaks generated at wavenumbers of 3636–3639 cm^{-1}, 1470 cm^{-1}, and 951–985 cm^{-1} indicate a specific phase, such as calcium hydroxide, calcium carbonate, and calcium silicate hydrate. The presence of sodium carbonate is indicated in the sample, which is immersed in CO_2-saturated brine. However, the carbonate peak appears in the hardened cement of PC60 and PC130. This suggests that during curing of cement, the atmospheric CO_2 is diffused through the cement matrix and reacts with carried pore water with a high concentration of sodium forming carbonates. Interestingly, Fig. 6 depicts the absence of calcium hydroxide peak in 24PC130b, 72PC130b, and 96PC130b at wave number 3636 cm^{-1}, which suggests that calcium hydroxide is totally consumed during carbonation.

Compressive strength, visual inspection and testing

The compressive strength of newly prepared geopolymer cement samples is tested. Figure 7 shows the visual inspection of Class G cement immersed in CO_2-brine saturated for 96 h in the autoclave (96GC130b). It is clearly noticed that there are two distinct zones situated in all sides of samples,
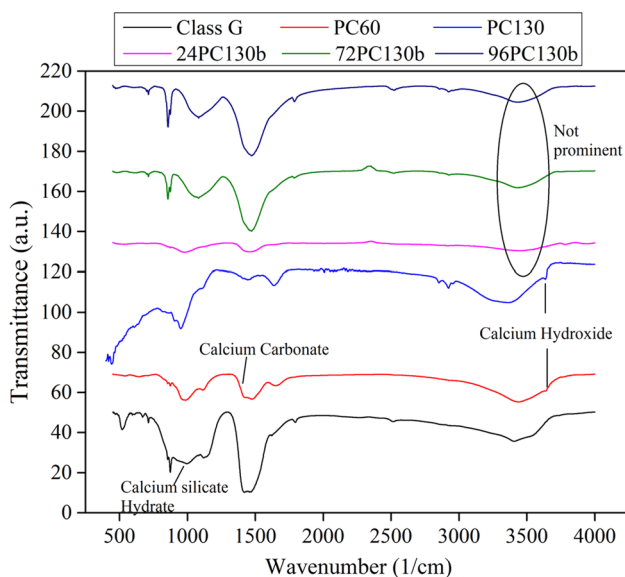
less 'gray' altered area (X) and heavy 'white' altered area (Y) by CO_2-saturated brine. The compressive strength of 96GC130b sample is 13.6 MPa, which is decreased up to approximately 64% from the strength before exposure to CO_2-saturated brine. Three samples are tested for each condition under the compression load. Furthermore, the analysis of cement sample microstructure, crystallinity and functional group is taken from the heavily altered area of the sample.

The impact of CO_2-saturated brine on the compressive strength of the cement after the exposure for 24, 72 and 96 h is presented in Fig. 8. Generally, the compressive strength of geopolymer cement pastes is higher compared to Class G cement pastes. It is observed that the compressive strength of geopolymer cement (GC) at 60 °C increases with the aging time. However, the opposite trend is observed for Class G cement at similar conditions. This phenomenon is also observed at 130 °C, which affirms the potential candidature of the newly prepared GC for CO_2 injection wells or wells with naturally rich CO_2 content. This is attributed to the fact that the increasing breakage of the glassy chain of the fly ash activates Si and Al, which is assisted by maintaining the temperature to accelerate strength development.

It is also observed that higher curing temperature leads to higher compressive strength for geopolymer cement. An increase in the curing conditions from 17.23 MPa/60 °C to 24.13 MPa/130 °C increases the compressive strength of approximately 100%. It can be attributed to the rapid geopolymerization process at an early stage, caused by higher curing temperature. In a similar situation for Class G cement, the sample experiences a 20% reduction in compressive strength when the temperature is increased from 60 °C to

Fig. 6 FTIR pattern of the Class G cement powder and Class G cement (PC) paste before and after exposed to CO2-saturated brine

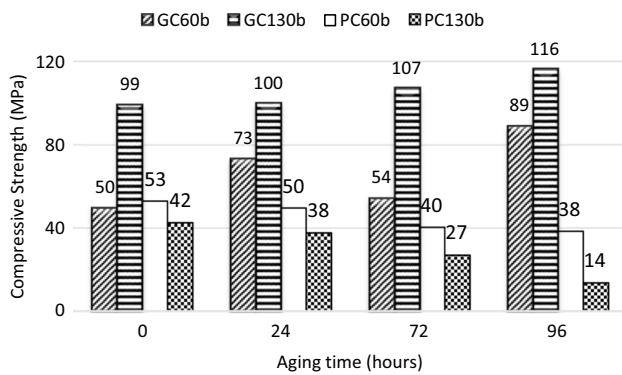**Fig. 7** API Class G cement after immersion test under CO_2-saturated brine

Fig. 8 Compressive strength of GC after CO_2-saturated brine exposure

130 °C. The compressive strength of GC60 is found to be 6.36% higher compared to PC60. Similarly, GC130 possesses compressive strength of 133.62% higher than PC130. The potential reason for this considerable strength difference is attributed to the reason that at elevated temperatures, alite and belite quickly hydrate and yield portlandite and C–S–H gel during the early stage of strength development, which act as an excellent compressive strength agent.

Conclusion

This research presents an experimental investigation into the effect of temperature on the microstructure and mechanical properties of fly ash geopolymer well cement immersed in CO_2-saturated brine. The strength of geopolymer cement increases at 60 °C and 130 °C, while the strength of Class G cement decreases as a function of exposure durations. It is found that the carbonation reaction of portlandite is mostly completed at 130 °C, resulting in the precipitation of calcium carbonate, which is later leached in the presence of carbonic acid, therefore causing loss of mechanical strength. The results from this research suggest that the concentration of CO_2 has a minor influence on the degree of carbonation. The temperature is found to be a more critical factor for microstructure and mechanical properties reduction in portland cement in a CO_2-rich environment. The compressive strength and microstructural characterization confirm that the maximum degradation occurs at 130 °C. Fly ash is potentially used as a binder in oil well cement for CO_2 injection wells or wells with naturally rich CO_2. Binder material is optimal if it has lower calcium content to suppress carbonation reactions. It can be achieved with hybrid cement, alkali-activated product by mixing fly ash with low calcium material such as metakaolin. Further studies can be carried out to investigate the potential and capabilities

of geopolymer cement immersed in CO_2-saturated brine at varying conditions of the desired depth of the oil well.

Oil well cementing with wellbore integrity is a crucial step in oil and gas industry and is considered as one of the foremost challenging operations in petroleum drilling. CO_2 management is one of the important procedures in Malaysian oil and gas drilling industry as it constitutes a huge level in the oil and gas underground reserves. This work is focused on such applications where the geopolymer cement is immersed in the CO_2-saturated brine at varying reservoir conditions. A complete understanding is required to assess the known and unknown behavior of geopolymer cement at different conditions. Therefore, the authors propose to expand the research toward a detailed experimental architecture at more elevated temperature and pressure conditions, and varying alkali/fly ash concentration ratio for more realistic approach toward deep wells applications.

Availability of data and material The data will be available on request.

Code availability Not applicable.

Declarations

Conflict of interest The authors declare no conflict of interest.

References

API Recommended Practice 10A. Specification for cements and materials for well cementing; 2011.

API Recommended Practice 10B-2. Recommended practice for testing well cements; 2009.

ASTM C 109/C 109M–07 A. Standard test method for compressive strength of hydraulic cement mortars; 2008.

Bakria AMM, Kamarudin H, Hussain M, Nizar IK, Zarina Y, Rafiza AR (2011) The effect of curing temperature on physical and chemical properties of geopolymers. Phys Procedia 22:286–291

Belmokhtar N, Ammari M, Brigui J, Benallal L (2017) Comparison of the microstructure and the compressive strength of two geopolymers derived from Metakaolin and an industrial sludge. Constru Build Mater 146:621–629

Chindaprasirt P, Rattanasak U, Taebuanhuad S (2013) Resistance to acid and sulfate solutions of microwave-assisted high calcium fly ash geopolymer. Mater Struct 46:375

Davidovits J (2011) Geopolymer chemistry and applications, 3rd edn. Institute Geopolymer

Duxson P, Fernández-Jiménez A, Provis JL, Lukey GC, Palomo A, van Deventer JSJ (2007) Geopolymer technology: the current state of the art. J Mater Sci 42:2917–2933

Fauzi A, Nuruddin MF, Malkawi AB, Abdullah MMAB (2016) Study of fly ash characterization as a cementitious material. Proc Eng 148:487–493

Jacquemet N, Pironon J, Lagneau V, Saint-Marc J (2012) Armoring of well cement in H_2S–CO_2 saturated brine by calcite coating—Experiments and numerical modelling. Appl Geochem 27:782–795

Junaid MT, Kayali O, Khennane A (2017) Response of alkali activated low calcium fly-ash based geopolymer concrete under compressive load at elevated temperatures. Mater Struct 50:50

Kaze CR, Alomayri T, Hasan A, Tome S, Lecomte-Nana GL, Nemaleu JGD, Tchakoute HK, Kamseu E, Melo UC, Rahier H (2020) Reaction kinetics and rheological behaviour of meta-halloysite based geopolymer cured at room temperature: effect of thermal activation on physicochemical and microstructural properties. Appl Clay Sci 196:105773

Khalifeh M, Saasen A, Vralstad T, Hodne H (2014) Potential utilization of Class C fly ash-based geopolymer in oil well cementing operations. Cement Concr Compos 53:10–17

Komnitsas K, Zaharaki D (2007) Geopolymerisation: a review and prospects for the minerals industry. Mineral Engineering 20:1261–1277

Kutchko BG, Strazisar BR, Lowry GV, Dzombak DA, Thaulow N (2008) Rate of CO_2 attack on hydrated Class H well cement under geologic sequestration conditions. Environ Sci Technol 42:6237–6242

Mahmoud AA, Elkatatny S, Mahmoud M. Improving Class G cement carbonation resistance using nanoclay particles for geologic carbon sequestration applications. Society of Petroleum Engineers. 2018; SPE-192901-MS.

Nuruddin MF, Demie S, Shafiq N (2011) Effect of mix composition on workability and compressive strength of self-compacting geopolymer concrete. Canadian J Civil Eng 38:1196–1203

Omosebi O, Maheshwari H, Ahmed R, Shah S, Osisanya S, Hassani S, DeBruijn G, Cornell W, Simon D (2016) Degradation of well cement in HPHT acidic environment: effects of CO_2 concentration and pressure. Cement Concr Compos 74:54–70

Omosebi OA, Sharma M, Ahmed RM, Shah SN, Saasen A, Osisanya SO. Cement degradation in CO_2–H_2S environment under high pressure-high temperature conditions. Society of Petroleum Engineers. 2017; SPE-185932-MS.

Palomo A, Grutzeck MW, Blanco MT (1999) Alkali-activated fly ashes: a cement for the future. Cem Concr Res 29:1323–1329

Phair JW, Van Deventer JSJ (2002) Effect of the silicate activator pH on the microstructural characteristics of waste-based geopolymers. Int J Miner Process 66:121–143

Ramezanianpour AA (2014) Cement replacement materials: properties, durability, sustainability. Springer, Heidelberg

Ridha S, Irawan S, Ariwahjoedi B (2013) Strength prediction of Class G oilwell cement during early ages by electrical conductivity. J Petrol Explor Prod Technol 3:303

Ridha S, Setiawan RA, Abd Hamid AI, Shahari AR (2018) The influence of CO_2 accelerated carbonation on alkali-activated fly ash cement under elevated temperature and pressure. Mater Sci Eng Technol (materialwissenschaft Und Werkstofftechnik) 49(4):483–548

Ridha S, Setiawan RA, Pramana AA, Abdurrahman M (2020) Impact of wet supercritical CO_2 injection on fly ash geopolymer cement under elevated temperatures for well cement applications. J Petroleum Explorat Prod Technol 10:243–247

Ridha S, Yerikania U. New nano-geopolymer cement system improves wellbore integrity upon acidizing job: experimental findings. Society of Petroleum Engineers. 2015; SPE-176419-MS.

Ryu GS, Lee YB, Koh KT, Chung YS (2013) The mechanical properties of fly ash-based geopolymer concrete with alkaline activators. Constr Build Mater 47:409–418

Santra AK, Reddy BR, Liang F, Fitzgerald R. Reaction of CO_2 with Portland cement at downhole conditions and the role of pozzolanic supplements. Soc Petrol Eng. 2009; SPE-121103-MS.

Sauki A, Irawan S (2010) Effects of pressure and temperature on well cement degradation by supercritical CO_2. Int J Eng Technol 10:53–61

Velayati A, Tokhmechi B, Soltanian H, Kazemzadeh E (2015) Cement slurry optimization and assessment of additives according to a proposed plan. J Natural Gas Sci Eng 23:165–170

Zhang L, Dzombak DA, Nakles DV, Hawthorne SB, Miller DJ, Kutchko BG, Lopano CL, Strazisar BR (2013) Characterization of pozzolan-amended wellbore cement exposed to CO_2 and H_2S gas mixtures under geologic carbon storage conditions. Int J Greenhouse Gas Control 19:358–368

Zhang Y, Xiao R, Jiang X, Li W, Zhu X, Huang B (2020) Effect of particle size and curing temperature on mechanical and microstructural properties of waste glass-slag-based and waste glass-fly ash-based geopolymers. J Clean Prod 273:122970